Development of a combined solver to model transport and chemical reactions in catalytic wall-flow filters

Allouche, Mohamed Hatem; Enjalbert, Romain; Alberini, Federico; Ariane, Mostapha; Alexiadis, Alessio

DOI:
10.1016/j.cherd.2016.11.014

Document Version
Peer reviewed version

Citation for published version (Harvard):
Allouche, MH, Enjalbert, R, Alberini, F, Ariane, M & Alexiadis, A 2017, 'Development of a combined solver to model transport and chemical reactions in catalytic wall-flow filters', *Chemical Engineering Research and Design*, vol. 117, pp. 681-687. https://doi.org/10.1016/j.cherd.2016.11.014

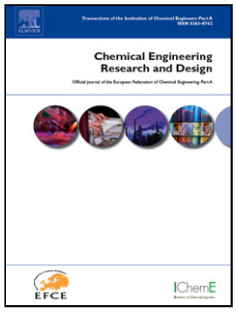

Title: Development of a Combined Solver to Model Transport and Chemical Reactions in Catalytic Wall-Flow Filters

Author: Mohamed Hatem Allouche Romain Enjalbert Federico Alberini Mostapha Ariane Alessio Alexiadis

PII: S0263-8762(16)30432-4
DOI: http://dx.doi.org/doi:10.1016/j.cherd.2016.11.014
Reference: CHERD 2485

To appear in:

Received date: 30-7-2016
Revised date: 27-10-2016
Accepted date: 14-11-2016

Please cite this article as: Allouche, Mohamed Hatem, Enjalbert, Romain, Alberini, Federico, Ariane, Mostapha, Alexiadis, Alessio, Development of a Combined Solver to Model Transport and Chemical Reactions in Catalytic Wall-Flow Filters.Chemical Engineering Research and Design http://dx.doi.org/10.1016/j.cherd.2016.11.014

Development of a Combined Solver to Model Transport and Chemical Reactions in Catalytic Wall-Flow Filters

Allouche Mohamed Hatem[a], Enjalbert Romain[b*], Alberini Federico[c], Ariane Mostapha[d], Alexiadis Alessio[c]

[a] INSA Euro-Méditerranée, Université Euro-Méditerranéenne de Fès, Fès, Morocco
[b] Veolia, London, United Kingdom
[c] School of Chemical Engineering, University of Birmingham, Birmingham, United Kingdom
[d] Laboratoire Interdisciplinaire Carnot de Bourgogne, Université de Bourgogne Franche-Comté, Dijon, France

Highlights

- We develop an exothermic model for diesel particulate filters.
- We consider both single-reaction and competing reactions systems.
- Isothermal models are adequate to describe the temperature and concentration profiles.
- Non-isothermal models are needed to determine the critical temperature.

Abstract

In this work, we develop a non-isothermal model for diesel particulate filters including exothermic and competing chemical reactions. We begin with an isothermal, single-reaction model and we gradually increase its complexity. By comparing various models, we aim at establishing the minimum degree of complexity required to effectively model the system under investigation. Based on the numerical simulations, we conclude that isothermal models are adequate only if the temperature of the catalyst is, at all times, completely below or completely above a critical temperature. However, if the goal is to predict the critical temperature, only non-isothermal models should be used. The results with competing reactions, on the other hand, show that the presence of competing reactions does not affect significantly the overall conversion in the filter.
Keywords: *CFD; reactive flow; heat and mass transfer; catalytic converter; Diesel particulate filter.*

Nomenclature

A	Pre-exponential Factor	
C	Concentration	[mol m^{-3}]
C_p	Specific Heat Capacity	[J $kg^{-1}K^{-1}$]
$[C_3H_6]$	Propene Concentration	[mol m^{-3}]
$[CO]$	Carbon Monoxide Concentration	[mol m^{-3}]
d	Darcy Coefficient	[m^{-2}]
D	Mass Diffusivity	[m^2s^{-1}]
E_A	Activation Energy	[J mol^{-1}]
F	Forchheimer Coefficient	[m^{-1}]
ΔH	Heat of Reaction	[J mol^{-1}]
k	Reaction Rate Constant	
K	Adsorption Rate Constant	
$\vec{n}$	Normal Vector	
$[O_2]$	Oxygen Concentration	[mol m^{-3}]
p	Pressure	[Pa]
r	Reaction rate	[mol $m^{-3}s^{-1}$]
R	Universal Gas Constant	[J $mol^{-1}K^{-1}$]
S	Heat Source	[K s^{-1}]
t	Time	[s]

T	Temperature	[K]
u	Velocity	[m s^{-1}]
$\mathbf{u_t}$	Tangential Component of the Velocity	[m s^{-1}]
α	Thermal Diffusivity	[m^2s^{-1}]
μ	Dynamic Viscosity	[Pa s]
ρ	Density	[kg m^{-3}]

1.0 Introduction

Regulations within the European Union and elsewhere encourage the development of solutions to abate vehicle emissions due to increasing environmental and health concerns [1], [2]. A wall-flow filter, also known as a diesel particulate filter, is a device installed at engine exhausts that captures soot in order to oxidize it as well as removing carbon monoxide (CO) and unreacted hydrocarbons [3].

Diesel particulate filters are monoliths in which the channels contain a porous region [4]. The porous region is embedded with catalyst to oxidize CO and hydrocarbons while acting as a trap for soot particles. During the so-called filter regeneration process, soot is oxidized [5], [6]. Thermodynamically, diesel soot oxidizes at temperatures above 600°C, however, the use of a catalyst can reduce this temperature significantly [7], [8].

Additionally to trapping and removing soot, diesel particulate filters oxidize carbon monoxide and hydrocarbons into carbon dioxide. Carbon monoxide is the dominant chemical reactant in the filter and, therefore, the overall performance of a diesel particulate filter is assessed mainly by measuring the conversion of this chemical species.

Recent works have been performed in order to obtain deeper insight into the soot loading process and analyse how diesel soot is deposited on the walls of the filter media. Chiavola et al. focuses on how soot profile evolves during engine operation in a specified duty cycle, starting from pre-loaded channels [9].

Falcucci aimed at presenting a global lumped parameter for onboard applications to estimate soot morphology and its effects on DPF performances. Indeed, the morphology of particulate matter influences the permeability of soot deposit inside the DPF: the growth of soot layer has a non negligible impact on the pressure and the temperature trend during the regeneration in the different zones of the DPF [10].

Di Sarli & Di Benedetto investigated the effect of the catalyst activity on the regeneration dynamics of the filter in the light of the thermal interaction between combustion of the soot in the (catalytic) porous wall and combustion of the cake [11]. The main results of this work show a transition from slow

(uniform combustion) to fast (front propagation) regeneration with increasing catalyst activity.
Di Sarli et al. studied recently the cake layer by investigating the effect of the soot-catalyst contact on the regeneration performance of a DPF wash-coated with nano-metric ceria particles [12]. By varying the catalyst/soot ratio, this study highlights the importance of strategies that avoid or minimize the segregation between the cake layer and the catalytic wall of the filter to operate catalyst-coated DPFs in an effective manner.

There are two main groups of filters: (i) flow-through filters where the porous wall is parallel to the gas flow direction, and (ii) wall-flow filters which are derived from flow-through filters where channel ends are alternatively plugged to force the gas flow through the porous walls. This work deals with wall flow-filters, which have the advantage of a lower light-off temperature (the temperature where 50% conversion is achieved).

As carbon monoxide oxidation is the dominant chemical reaction, we need to determine its reaction kinetic. The Langmuir-Hinshelwood kinetic is the most commonly accepted reaction mechanism [13], [14]. Beside the reaction mechanism, in non-isothermal conditions, the chemical reaction is also characterized by its activation energy. Values for the activation energy are available in literature, depending on the type of catalyst used. For palladium catalysts, these values are in the range 70–110 kJ mol^{-1} [15], [16]; for platinum catalysts, they are in the range 55–140 kJ mol^{-1} [16]–[18].

In this work, we model the hydrodynamics, mass transport, and chemical reactions occurring in a clean diesel particulate filter. The flow in both the external and the porous region is accounted for, and the reacting chemicals are described by transport equations. Contrary to previous studies (e.g. [7], [19]), which only account for isothermal models, in this work the heat generated by the exothermic reactions is considered and coupled to the flow dynamics and the reaction constants. We also study the case of competing reactions, where carbon monoxide competes for access to the catalyst surface with unreacted hydrocarbons.

We begin with the single-reaction isothermal model and we gradually increase its complexity by adding competing and exothermic reactions. Ultimately, the goal is to assess if common isothermal models commonly used in literature (e.g. [7], [19]) are adequate to describe the conversion profiles inside the filter, or more complex models are required. In the latter case, by comparing models with various levels of complexity, we also aim at establishing the minimum degree of complexity required to effectively model the system under investigation.

2. Model and equations

This section specifies the geometry of the channel, as well as the information regarding the feed and the chemical reactions taking place.

2.1 Geometry

The system is a channel from a wall-flow filter describing a clean diesel particulate filter (figure 1a). Figure 1b shows the simulated geometry corresponding to a 2D symmetric slice; the dashed line represents a symmetry line that will be used as a boundary condition, while the dashed area is the porous region. The flow follows the direction of the arrows. Table 1 provides the dimensions of the system, as they are labelled in figure 1b.

Two different feeds are analysed within this work (see Section 2.2). They represent two typical simplifications that can be used to describe the feed, and related chemical reactions, of a diesel particulate filter.

2.2 Chemical reaction

Two simplified kinetic models will be considered in this work: the single reaction model and the competing reaction model.

2.2.1 Single reaction model

The first model describes a simple carbon monoxide oxidation. Feed 1 in Table 2 provides the feed for this system. From the feed information and the stoichiometry of the reaction, we can verify that oxygen is overabundant in the feed. This means that there is more than enough oxygen to convert all the reactants in the filter.
The chemical reaction ($CO + 0.5O_2 \rightarrow CO_2$) rate is given by

$$r_1 = \frac{k_1[CO][O_2]}{(1+K_1[CO])^2} \ . \qquad (1)$$

The relation between the kinetic parameters k_1 and K_1 and temperature is described by the Arrhenius equation,

$$k_i = Ae^{\frac{-E_A}{RT}} \ , \qquad (2)$$

where A is the pre-exponential factor, E_A is the activation energy and R is the universal gas constant.

Table 3 provides chemical values related to equation 2. Additionally, the heat of reaction for carbon monoxide oxidation is -283 kJ mol^{-1} [18].

2.2.2 Competing reaction model

The second model accounts for the additional chemical reaction of propene oxidation ($C_3H_6 + 4.5O_2 \rightarrow 3CO_2 + 3H_2O$). Feed 2 in Table 2 provides the feed for this system. The difference with the previous feed is the addition of propene. Also in this case, the feed is still oxygen rich; therefore the all the carbon monoxide and propene present in the feed can be oxidized.

The chemical reaction rates are given by

$$r_1 = \frac{k_1[CO][O_2]}{(1+K_1[CO]+K_2[C_3H_6])^2} \qquad (3)$$

and

$$r_2 = \frac{k_2[C_3H_6][O_2]}{(1+K_1[CO]+K_2[C_3H_6])^2} \ . \qquad (4)$$

It is important to note that the equation describing the carbon monoxide oxidation is different when propene is present in the system. This is due to the propene competing for the adsorption on the catalyst.

The reaction rate constants are temperature dependent and follow Arrhenius' equation (eq. 2). Pre-Exponential Factor and Activation Energy are given in Table 3. The heat of reaction for propene oxidation is 2,044 kJ mol^{-1} [18].

For both Feed 1 and Feed 2, the porous region contains the catalyst where the chemical reaction occurs. Outside of the porous region, the reaction rate is assumed negligible.

2.3 Modelling

The "simplePorousFoam" solver has been chosen in the implicit form that is appropriate for steady-state problems. It is an incompressible solver that contains the Navier-Stokes equation, the continuity equation, the Darcy-Forcheimmer law and a utility to define the porous region where the Darcy-Forcheimmer law will be applied.
To ensure stability, the time scheme is sometimes changed to a Euler numerical scheme, whilst the Laplacian scheme switches to a Gauss linear uncorrected scheme. However, when the Euler scheme is used the steady-state solution is not the default solution. Therefore, in order to ensure that the system has reached a steady state, a long end time is defined in the solver. The solution is then observed at different times, and only long after the solution ceases to change with time, is the steady state assumed.
The discussed chemical reaction rates are integrated with the fluid dynamics equations in order to fully model the system. In the range of gas flow velocities considered in this study, the Reynolds number based on the thickness of the porous layer is of the order of unity, and the Mach number tends to zero. This means that the flow can be assumed laminar and incompressible. The fluid dynamics is described by the Navier-Stokes equation

$$\rho\left(\frac{\partial \boldsymbol{u}}{\partial t} + \boldsymbol{u}\cdot\nabla\boldsymbol{u}\right) = -\nabla p + \mu\nabla^2\boldsymbol{u} \qquad (5)$$

and the continuity equation.

$$\frac{\partial \rho}{\partial t} + \nabla \cdot (\rho \boldsymbol{u}) = 0, \qquad (6)$$

where ρ and μ are the gas density and dynamic viscosity, $\boldsymbol{u}$ is the velocity field, and p is the pressure. Equations 5 and 6 are solved for transient flow. The external pressure is assumed to be atmospheric, as the pressure drop is small and the exhausted gas is released to the environment [7].

For the fluid motion within the porous region, we use the Darcy-Forchheimer law

$$-\nabla p = \mu \boldsymbol{u} d + \frac{1}{2} \rho \boldsymbol{u}^2 F\,, \qquad (7)$$

which is enforced only in the porous region of the system (see figure 1).

Due to the low velocity, the Forchheimer term, *F*, is negligible and the equation simplifies to the Darcy's law. The Darcy's coefficient *d*, in this case, is $1.6 \cdot 10^{12}$ m^{-2} [20].

The concentration of the various chemical species is included in the balance equation for the generic chemical species *C*

$$\frac{\partial C}{\partial t} = -\nabla \cdot (\boldsymbol{u} C) + D \nabla^2 C + r\,. \qquad (8)$$

One scalar transport equation is implemented for each reactant *C*, and *r* is the corresponding source term coming from the chemical reaction of species *C*.

The diffusion coefficient can be considered the same for all chemical species and constant with temperature and set to $D=10^{-6}$ $m^2 s^{-1}$ [7].

In the non-isothermal simulations, we also include the energy balance equation

$$\frac{\partial T}{\partial t} = -\boldsymbol{u} \cdot \nabla T + \alpha \nabla^2 T + S\,, \qquad (9)$$

where *T* is the temperature, α is the heat diffusivity of the gas and *S* the source term that describes the heat generated by the exothermic reactions within the filter. The source term is given by

$$S = \frac{\Delta H}{\rho C_p} r, \qquad (10)$$

where C_p is the specific heat capacity and ΔH is the heat of reaction. Previous studies show that the parameters in equation 10 can be considered constant in the range of temperature under investigation [7].

Table 4 provides the boundary conditions implemented (figure 1b). The lines L_9 and L_{10} indicate the separation between the continuous and the porous domain and do not require any special boundary condition.

The inlet gas velocities used in the simulations are between 0.05 and 0.2 ms^{-1}; inlet temperatures between 423K and 623K.

3. Results and Discussion

3.1 Mesh independency and model accuracy

Computational fluid dynamics (CFD) calculations are carried out with OpenFOAM. In most of the simulations, the time step was in the range between 1 and 0.1 s. Non-isothermal simulations, with competing reactions, at high gas velocities, where the light-off temperature is reached within the filter, however, require smaller time steps around 10^{-5} s. In this case, the smaller time steps are coupled with the more stable numerical schemes. Results calculated with various structured square/rectangular meshes are compared to determine mesh independence. Figure 2 shows the case of Feed 1 with V = 0.1 m s^{-1} and T = 525 K. Carbon monoxide conversion reaches a plateau for meshes with more than 10 000 cells.

In order to verify the accuracy of our model, we compared our results with those of Knoth et al. [7]. They studied a three times longer channel and used steady-state isothermal flow. The CO concentration in the feed was 500 ppm and the inlet velocity 0.1 m s^{-1}.

Figure 3 illustrates the relationship between carbon monoxide conversion and inlet temperature. The graph shows that the results of Knoth et al. [7] and those obtained with our model are almost identical. The slight discrepancy between the two data can be explained by the different numerical approach. Knoth et al. [7] used COMSOL™, based on finite elements, while we used OpenFOAM based on finite volumes.

3.2 Single Reaction Model (isothermal)

The model is applied to the geometry described in figure 1. Initially, the energy equation is deactivated. The model, therefore, becomes isothermal like previous studies (e.g. [7], [19]). We proceed in this way because we want to begin with the simplest situation and gradually increase the complexity of the model. The final goal is to compare models of various features and establish the minimum level of complexity required to effectively model the filter.

Figure 4 displays the relationship between temperature and carbon monoxide conversion at different inlet velocities. This result points out that inlet velocity has an impact on the CO conversion. In particular, the light-off temperature decreases with the inlet velocity.

3.3 Competing Reaction Model (isothermal)

In this section, the model is improved by considering the presence of both carbon monoxide and propene, but still at isothermal conditions.

A variety of hydrocarbons at low concentrations compose the actual inlet of the filter. However, it is beyond the scope of this study to implement all the possible chemical species and chemical reactions that can actually occur in the filter, no matter how small their concentration. For simplicity, therefore, we lump all hydrocarbons together, and we add to the inlet 1% of propene, which is a typical reactant in the feed.

Two scenarios are possible: independent conversion of each reactant (figure 5), or competitive conversion (figure 6). The competition between propene and carbon monoxide does not concern oxygen, which is in excess, but access to the catalyst surface. Mathematically, this can be seen in the $[C_3H_6]$ term in equation (3) and in the [CO] term in equation 4.

Figure 5 displays the conversion of both carbon monoxide and the propene as a function of temperature, for an inlet velocity of 0.1m s^{-1}. Propene follows the same trend as the carbon monoxide, although the conversion has a small lag behind. This can be explained by propene oxidation having higher activation energy than carbon monoxide oxidation, and, therefore, requiring a higher temperature for the chemical reaction to reach similar conversions.

Figure 6 compares the conversion of the single reaction model with that of the competing reaction model. When competing reactions are considered, an additional term is added to the denominator of the carbon monoxide reaction rate (equation 3). However, figure 6 shows two almost identical profiles. Therefore, this extra term seems not to affect the final conversion.

3.4 Exothermic Single Reaction Model

As observed with the single and competing reactions, the temperature appears to have a dominant effect on the flow filter performance. However, until now, the system is isothermal. In principle, however, this assumption is not correct, as carbon monoxide oxidation and propene combustion are exothermic reactions, and increase the temperature of the system.

Therefore, we add the energy balance equation in our model. This was implemented only in the single reaction model, since, as shown in figure 6, the single and the competitive reaction models bring to small differences in terms of overall carbon monoxide conversion. The heat losses to the environment have been ignored due to the small contact area between the system and the exterior.

Figure 7 plots the temperature against the conversion at different velocities. It can be seen that in the non-isothermal case, the difference between the conversion curves calculated at different velocities is lower (compare to the isothermal case in figure 4). This can be explained by the coupling of the chemical reaction with the energy balance equation. As the reaction takes place, heat is generated which in turn fuels the chemical reaction, generating more heat. As a consequence, the impact of the inlet velocity on the final conversion is reduced and, when the reaction starts, it quickly goes to completion.

Figure 8 compares the conversion calculated with the non-isothermal model with that calculated with the isothermal model. We can determine a clear distinction between two states of the filter: (i) an "off" state at low temperatures where conversions are negligible, and (ii) an "on" state at higher temperatures where we have almost complete conversion. This behaviour appears in both the isothermal and exothermal models, but in the latter the switch between the "on" and "off" states is sharper and occurs at lower temperatures. In the non-isothermal case, we can identify a *critical temperature* that switches the state of the reactor from off to on.

3.5 Concentration and temperature profiles inside the filter

So far, we have discussed the final conversion of the filter once steady-state has been reached. In this section, we focus on the local concentration and temperature profiles that occur inside the filter. Figures 9 through 11 display the concentrations and temperatures at the centreline of the porous region (the dotted line in figure 1b).

Figure 9 shows how the system behaves at an inlet temperature of 493K, which is lower than the critical temperature. The chemical reactions never switch on and conversion is very low. The temperature along the filter remains almost constant and the concentration of CO only decreases slightly.
Figure 10 is similar to Figure 9, but the inlet temperature is now 503K, which is slightly lower than the critical temperature. In this case, the chemical reaction switches on inside the filter. We can distinguish two separate sections: (i) an "off-section" with low temperatures and high concentrations, and (ii) an "on-section" with high temperatures and low concentrations. This is shows that the coupling of the reaction terms with the energy balance equation is critical for the modelling of the filter.

Figure 11 shows the filter when the inlet temperature is above the critical temperature. As expected, at this temperature the reaction is on and it starts immediately to consume CO and produce heat. In theory, after CO has fully reacted, the temperature should decrease because no additional heat is produced. Figure 11 actually shows a little maximum at around 2 cm from the inlet. However, the high thermal conductivity of the gas ensures that the rest of the filter remains at almost isothermal conditions.

7.0 Conclusion

This paper develops an exothermic model that accounts for heat generation and the effect of temperature on the reaction constants. As the temperature appears to be a dominant factor, energy released by the exothermic reactions is taken into account, making our model more general than previous isothermal models. Isothermal models, in particular, do not have the ability to determine the critical temperature that *switches on* the temperature-dependant chemical reactions in the filter.

By comparing models with various levels of complexity (isothermal, non-isothermal, simple reaction, competing reactions), this study establishes the minimum degree of complexity required to effectively model a diesel particulate filter.

Our results show that isothermal models are in general adequate to describe the temperature and the concentration profiles inside the filter when the following two conditions are met: (i) we know in advance the critical temperature of the system, and (ii) the temperature of the catalyst is, at all times, completely below or completely above the critical temperature.

However, if the goal is to predict the critical temperature that switches on the filter, only non-isothermal models should be used. Additionally, non-isothermal models are superior also in cases when the critical temperature is attained within the reactor, in such a way that part of the reactor is above the critical temperature and part below.

Simulations carried out with and without competing reactions, on the other hand, do not show a significant difference of overall conversion in the filter.

The practical conclusion of this work is that researchers have a variety of modelling approaches for catalytic wall-flow filters. In this work, we identified the cases where more complex models are necessary and the cases where they are unnecessary. This is going to play a particularly important role for extensive 3D models requiring high computational resources. Being able of identifying the circumstances where the heat conservation equation is not fundamental can save considerable computational time allowing the simulation of larger systems.

References

[1] I. M. Kennedy, 'The health effects of combustion-generated aerosols', *Proceedings of the Combustion Institute*, vol. 31, no. 2, pp. 2757–2770, 2007.

[2] T. Tzamkiozis, L. Ntziachristos, and Z. Samaras, 'Diesel passenger car PM emissions: From Euro 1 to Euro 4 with particle filter', *Atmospheric Environment*, vol. 44, no. 7, pp. 909–916, 2010.

[3] A. G. Konstandopoulos and E. Papaioannou, 'Update on the Science and Technology of Diesel Particulate Filters', *KONA Powder and Particle Journal*, vol. 26, pp. 36–65, 2008.

[4] Ronald M. Heck and Robert J. Farrauto., *Catalytic air pollution control — Commercial Technology*. New York, 1995.

[5] A. M. Stamatelos, 'A review of the effect of particulate traps on the efficiency of vehicle diesel engines', *Energy Conversion and Management*, vol. 38, no. 1, pp. 83–99, 1997.

[6] C. Weaver, 'Particulate Control Technology and Particulate Standards for Heavy Duty Diesel Engines', *SAE Paper*, no. 840174, p. 19, 1984.

[7] J. F. Knoth *et al.*, 'Transport and reaction in catalytic wall-flow filters', *Catalysis Today*, vol. 105, no. 3–4, pp. 598–604, 2005.

[8] S.-J. Lee, S.-J. Jeong, and W.-S. Kim, 'Numerical design of the diesel particulate filter for optimum thermal performances during regeneration', *Applied Energy*, vol. 86, no. 7–8, pp. 1124–1135, 2009.

[9] O. Chiavola, G. Falcucci, and G. Chiatti, 'DPF Soot Profile Features Accounting for Engine Duty Cycle', *ASME*, pp. 177–185, 2006.

[10] G. Falcucci, 'A lumped parameter model for diesel soot morphology evaluation and emission control', *Proc. Inst. Mech. Eng. Part J. Automob. Eng.*, vol. 226, no. 7, pp. 987–998, 2012.

[11] V. Di Sarli and A. Di Benedetto, 'Modeling and simulation of soot combustion dynamics in a catalytic diesel particulate filter', *Chem. Eng. Sci.*, vol. 137, pp. 69–78. 2015.

[12] V. Di Sarli, G. Landi, L. Lisi, A. Saliva, and A. Di Benedetto, 'Catalytic diesel particulate filters with highly dispersed ceria: Effect of the soot-catalyst contact on the regeneration performance', *Appl. Catal. B Environ.*, vol. 197, pp. 116–124, 2016.

[13] M. Kawai, T. Onishi, and K. Tamaru, 'Oxidation of CO on a Pd surface: application of IR-RAS to the study of the steady state surface reaction', *Applied Surface Science*, vol. 8, no. 4, pp. 361–372, 1981.

[14] X. Zhou, Y. Barshad, and E. Gulari, 'Co oxidation on Pd/Al2O3. Transient response and rate enhancement through forced concentration cycling', *Chemical Engineering Science*, vol. 41, no. 5, pp. 1277–1284, 1986.

[15] S. Fuchs, T. Hahn, and H.-G. Lintz, 'The oxidation of carbon monoxide by oxygen over platinum, palladium and rhodium catalysts from 10−10 to 1 bar', *Chemical Engineering Process*, vol. 33, no. 5, pp. 363–369, 1994.

[16] P. J. Berlowitz, C. H. F. Peden, and D. W. Goodman, 'Kinetics of carbon monoxide oxidation on single-crystal palladium, platinum, and iridium', *Journal of Physical Chemistry*, vol. 92, no. 18, pp. 5213–5221, 1988.

[17] R. H. Venderbosch, W. Prins, and W. P. M. van Swaaij, 'Platinum catalyzed oxidation of carbon monoxide as a model reaction in mass transfer

measurements', *Chemical Engineering Science*, vol. 53, no. 19, pp. 3355–3366, 1998.

[18] S. E. Voltz, C. R. Morgan, D. Liederman, and S. M. Jacob, 'Kinetic Study of Carbon Monoxide and Propylene Oxidation on Platinum Catalysts', *Industrial Engineering Chemistry and Product Research and Development*, vol. 12, no. 4, pp. 294–301, 1973.

[19] M. Votsmeier, J. Gieshoff, M. Kögel, M. Pfeifer, J. F. Knoth, A. Drochner, and H. Vogel, 'Wall-flow filters with wall-integrated oxidation catalyst: A simulation study', *Applied Catalysis B: Environmental*, vol. 70, no. 1–4, pp. 233–240, 2007.

[20] K. Vafai, *Handbook of Porous Media, Second Edition*, CRC Press. 2005.

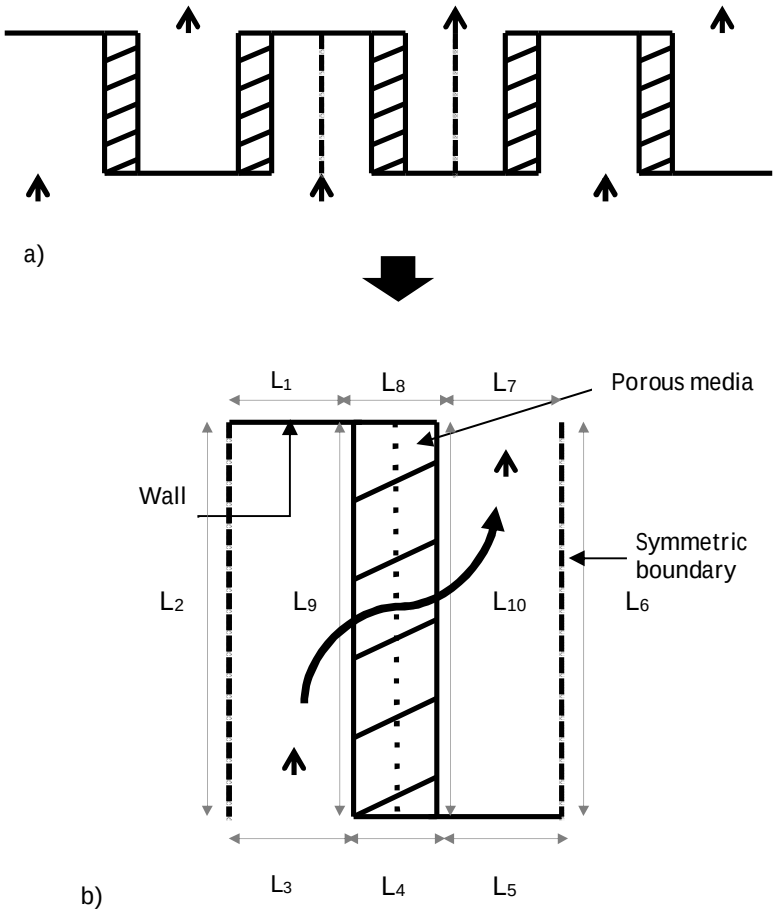

Figure 1 Schematic representation of the whole system (a) and the section used for the simulations (b).

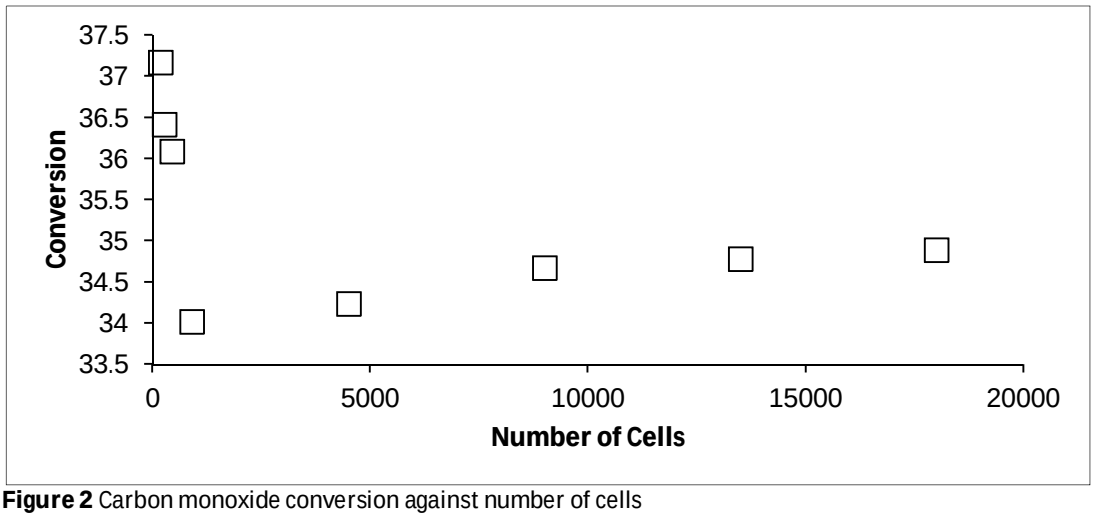

Figure 2 Carbon monoxide conversion against number of cells

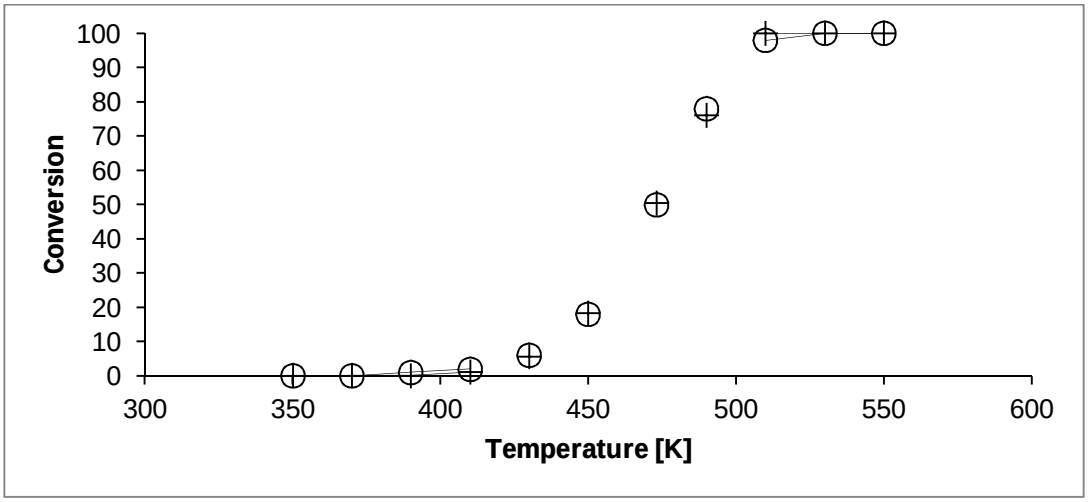

Figure 3 CO Conversion against temperature: comparison between our model (+) and Knoth et al. [7] (o).

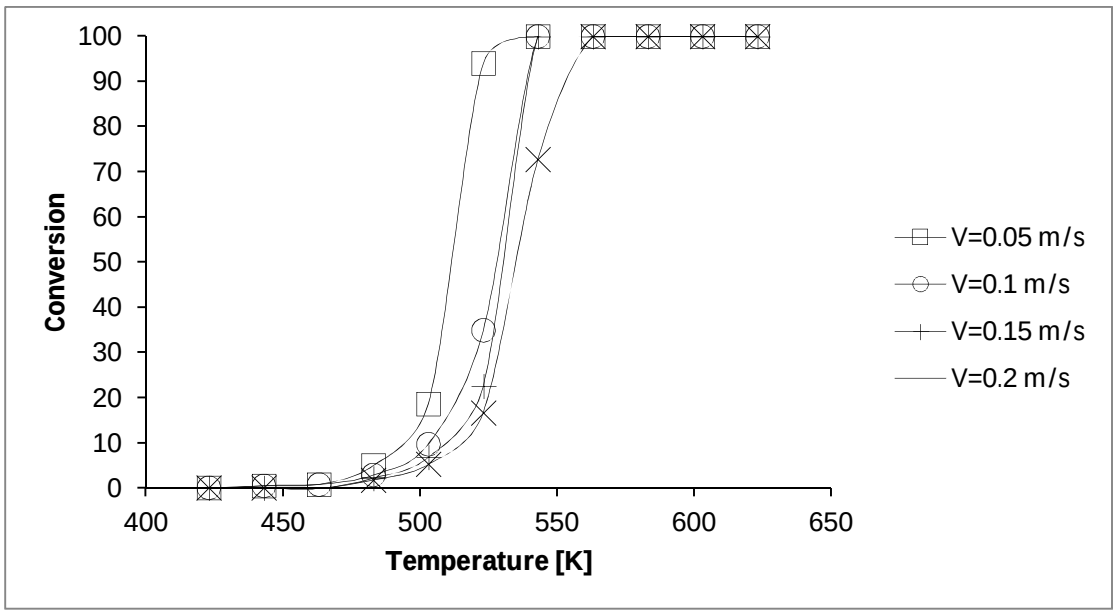

Figure 4 CO Conversion against temperature at different inlet gas flow velocities

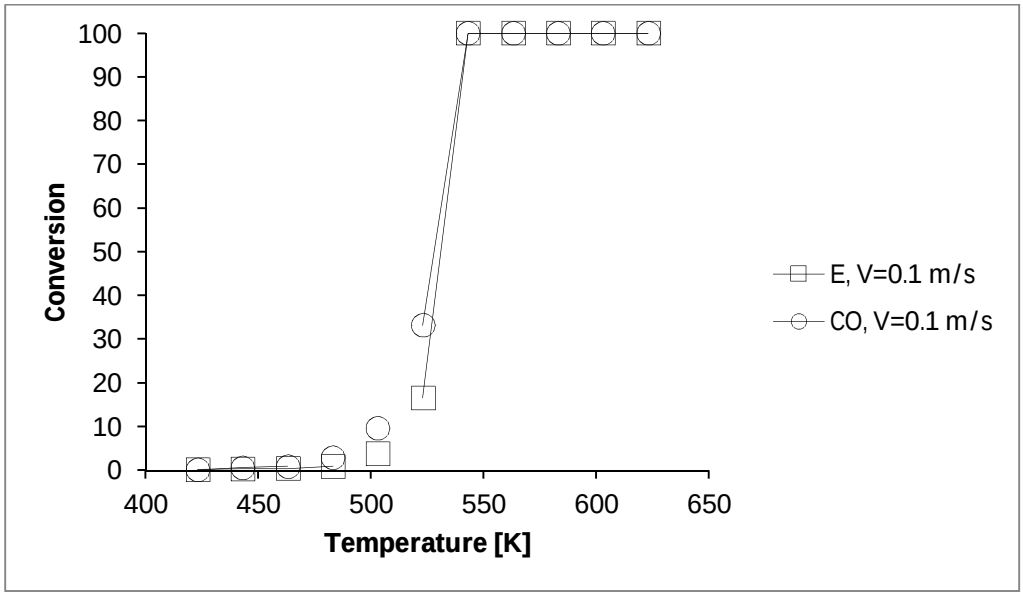

Figure 5 Conversion of carbon monoxide (CO) and propene (E) at 0.1m s^{-1}

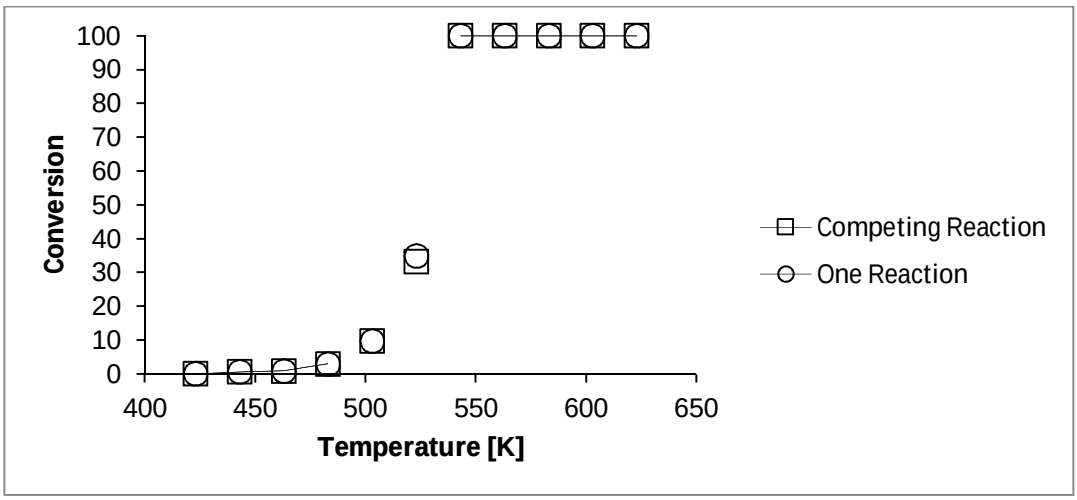

Figure 6 Conversion of carbon monoxide as function of temperature for single and competing reaction at 0.1m s^{-1}

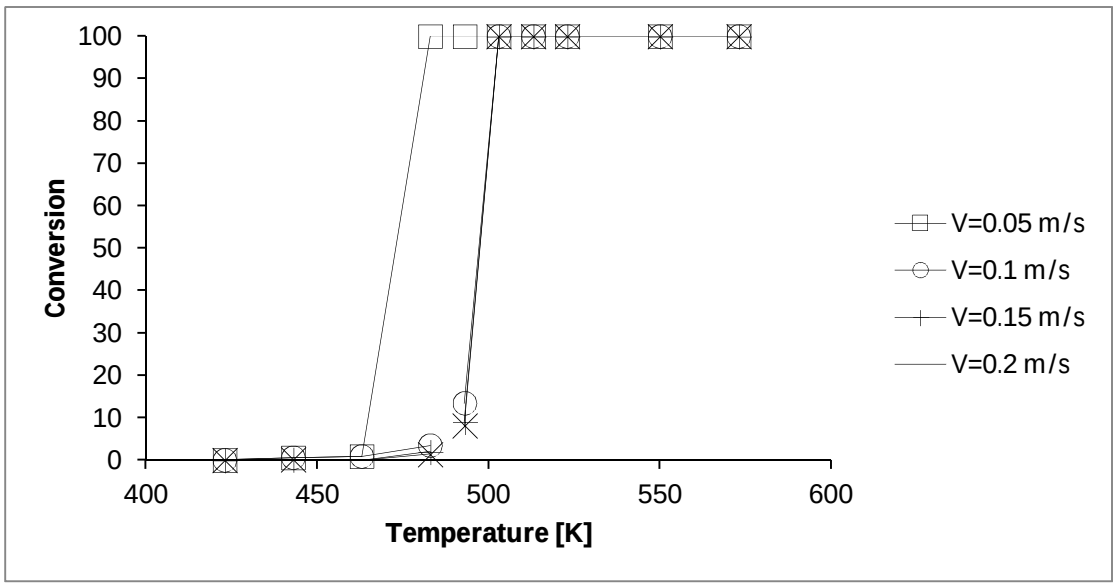

Figure 7 Carbon monoxide conversion as a function of temperature at different inlet velocities

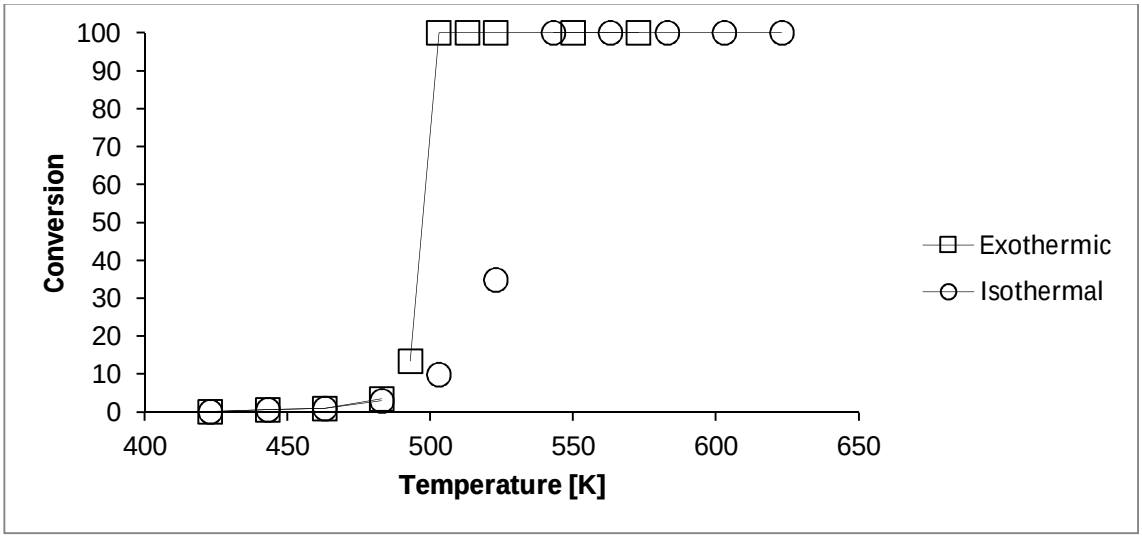

Figure 8 CO conversion as function of temperature for isothermal and non-isothermal system at 0.1ms^{-1}

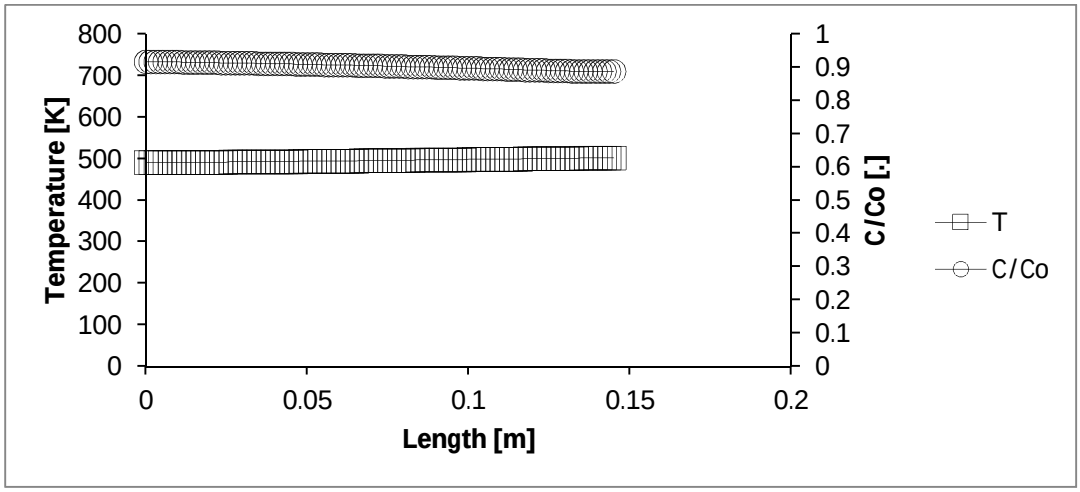

Figure 9 Temperature and dimensionless concentration of carbon monoxide through the centreline of the porous region (inlet velocity and temperature at respectively at 0.15 m s^{-1} and 493 K).

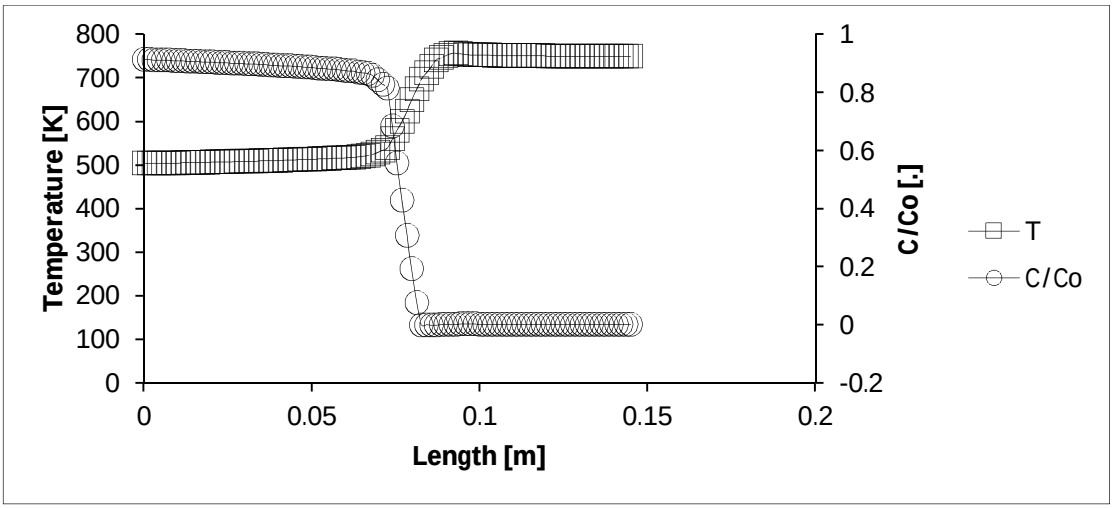

Figure 10 Temperature and dimensionless concentration of carbon monoxide through the centreline of the porous region (inlet velocity and temperature at respectively at 0.15 m s^{-1} and 503 K)

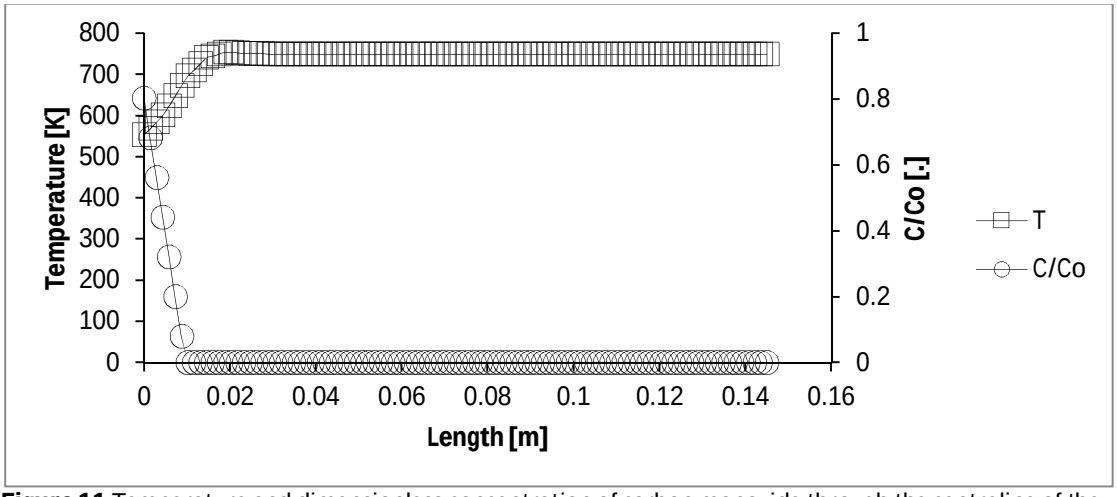

Figure 11 Temperature and dimensionless concentration of carbon monoxide through the centreline of the porous region (inlet velocity and temperature at respectively at 0.15 m s^{-1} and 523 K)

Table 1 Dimensions for Figure 1

L_1, L_3, L_5 and L_7 [cm]	L_4 and L_8 [cm]	L_2 L_9 L_{10} and L_6 [cm]
0.055	0.02	14.5

Table 2 Feed compositions for different systems

	N_2 [mol%]	**O_2 [mol%]**	**H_20 [mol%]**	**CO_2 [mol%]**	**CO [mol%]**	**C_3H_6 [mol%]**
Feed 1	76	10	5	5	4	0
Feed 2	75	10	5	5	4	1

Table 3 Arrhenius equation values according to [18]

	Pre-Exponential Factor	**Activation Energy kJ mol^{-1}**
k_1	$1.83 \cdot 10^{12}$ m^3 kmol^{-1} s^{-1}	104,393
k_2	$3.8 \cdot 10^{13}$ m^3 kmol^{-1} s^{-1}	121,090
K_1	$6.55 \cdot 10^{-1}$ m^3 kmol^{-1}	-14,400
K_2	$2.08 \cdot 10^{-3}$ m^3 kmol^{-1}	-5,400

Table 4 Boundary conditions fort the problem described by equations (5-9).

Eq.	**L_1**	**L_2**	**L_3**	**L_4**	**L_5**	**L_6**	**L_7**	**L_8**
5-6	u=0	$\vec{u} \cdot \vec{n} = \partial u_t / \partial \vec{n} = 0$	$u = u_{inlet}$	$\nabla u \cdot \vec{n} = 0$	u=0	$\vec{u} \cdot \vec{n} = \partial u_t / \partial \vec{n} = 0$	p=0 (p_{outlet})	$\nabla u \cdot \vec{n} = 0$
8	$\nabla C = 0$	$\nabla C \cdot \vec{n} = 0$	$C = C_{inlet}$	$\nabla C = 0$	$\nabla C = 0$	$\nabla C \cdot \vec{n} = 0$	$C = C_{outlet}$	$\nabla C = 0$
9	$\nabla T = 0$	$\nabla T .= 0$	$T = T_{inlet}$	$\nabla T = 0$	$\nabla T = 0$	$\nabla T \cdot \vec{n} = 0$	$T = T_{outlet}$	$\nabla T = 0$